Coupling Between $GABA_A$-R Ligand-Binding Activity and Membrane Organization in β-Cyclodextrin-Treated Synaptosomal Membranes from Bovine Brain Cortex: New Insights from EPR Experiments

Anahí V. Turina, Shirley Schreier & María A. Perillo

Cell Biochemistry and Biophysics

ISSN 1085-9195

Cell Biochem Biophys
DOI 10.1007/s12013-012-9338-1

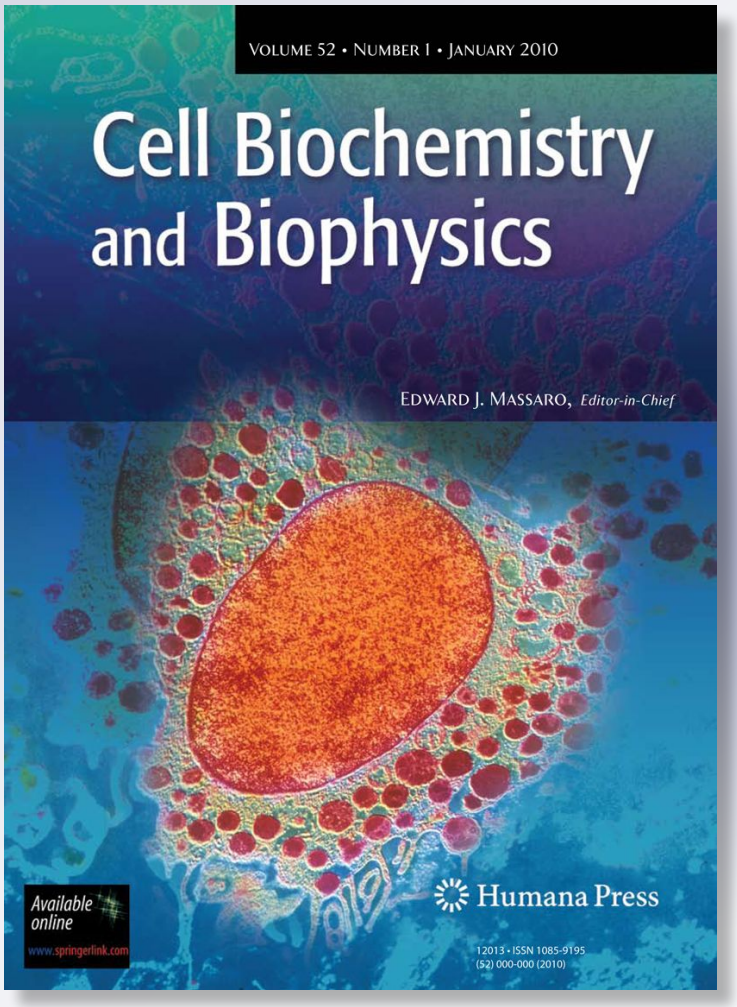

Springer

Cell Biochem Biophys
DOI 10.1007/s12013-012-9338-1

ORIGINAL PAPER

Coupling Between $GABA_A$-R Ligand-Binding Activity and Membrane Organization in β-Cyclodextrin-Treated Synaptosomal Membranes from Bovine Brain Cortex: New Insights from EPR Experiments

Anahí V. Turina · Shirley Schreier · María A. Perillo

Abstract Correlations between $GABA_A$ receptor ($GABA_A$-R) activity and molecular organization of synaptosomal membranes (SM) were studied along the protocol for cholesterol (Cho) extraction with β-cyclodextrin (β-CD). The mere pre-incubation (PI) at 37°C accompanying the β-CD treatment was an underlying source of perturbations increasing [^{3}H]-FNZ maximal binding (70%) and K_d (38%), plus a stiffening of SMs' hydrocarbon core region. The latter was inferred from an increased compressibility modulus (K) of SM-derived Langmuir films, a blue-shifted DPH fluorescence emission spectrum and the hysteresis in DPH fluorescence anisotropy (A_{DPH}) in SMs submitted to a heating–cooling cycle (4–37–4°C) with $A_{DPH,heating} < A_{DPH,cooling}$. Compared with PI samples, the β-CD treatment reduced B_{max} by 5% which correlated with a 45%-decrement in the relative Cho content of SM, a decrease in K and in the order parameter in the EPR spectrum of a lipid spin probe labeled at C5 (5-SASL), and significantly increased $A_{TMA\text{-}DPH}$. PI, but not β-CD treatment, could affect the binding affinity. EPR spectra of 5-SASL complexes with β-CD-, SM-partitioned, and free in solution showed that, contrary to what is usually assumed, β-CD is not completely eliminated from the system through centrifugation washings. It was concluded that β-CD treatment involves effects of at least three different types of events affecting membrane organization: (a) effect of PI on membrane annealing, (b) effect of residual β-CD on SM organization, and (c) Cho depletion. Consequently, molecular stiffness increases within the membrane core and decreases near the polar head groups, leading to a net increase in $GABA_A$-R density, relative to untreated samples.

Keywords Cyclodextrin · $GABA_A$ receptor · EPR · Fluorescence anisotropy · Langmuir films

Abbreviations

β-CD	β-Cyclodextrin
B_{max}	Maximal binding
BSA	Bovine serum albumin
CD-PI	Synaptosomal membranes treated with β-CD
Cho	Cholesterol
CON-PI	Synaptosomal membranes submitted to the pre-incubation necessary for the β-CD-mediated Cho extraction but in absence of β-CD
DPH	1,6-diphenyl-1,3,5-hexatriene
CSM	Center of spectral mass
DZ	Diazepam
EPR	Electron paramagnetic resonance
FNZ	Flunitrazepam
I	Immobile (protein bound) component in 12-SASL EPR spectra
K	Compressibility modulus

Electronic supplementary material The online version of this article (doi:10.1007/s12013-012-9338-1) contains supplementary material, which is available to authorized users.

A. V. Turina · M. A. Perillo (✉)
IIBYT, CONICET - Biofísica-Química, Departamento de Química, Facultad de Ciencias Exactas, Físicas y Naturales, Universidad Nacional de Córdoba, Av. Vélez Sarsfield 1611, 5016 Córdoba, Argentina
e-mail: mperillo@efn.uncor.edu

A. V. Turina
e-mail: aturina@efn.uncor.edu

S. Schreier
Departamento de Bioquímica, Instituto de Química, Universidade de São Paulo, Av. Prof. Lineu Prestes 748, São Paulo 05508-900, Brazil
e-mail: schreier@iq.usp.br

Published online: 04 February 2012

K_d	Equilibrium dissociation constant
Lo	Liquid-ordered phase
M	Mobile component (partitioned in the lipid phase) in 12-SASL EPR spectra
MF	Membrane-free
PI	Pre-incubation
$GABA_A$-R	$GABA_A$ receptor
SEM	Standard error of the mean
SM	Synaptosomal membranes
12-SASL	12-doxylstearic acid spin label
5-SASL	5-doxylstearic acid spin label
So	Solid-ordered phase
TMA-DPH	1-(4-trimethylammoniumphenyl)-6-phenyl-1,3,5-hexatriene *p*-toluenesulfonate

Introduction

The natural steroid cholesterol (Cho) is one of the main components of mammalian membranes. Different neurobiological roles have been attributed to Cho because it is a precursor in the cascade of steroid hormone formation. Moreover, the capacity of Cho to work as a buffer of membrane microviscosity and to modulate some functions of membrane proteins has been well recognized [1].

The modulation of integral membrane proteins could be due to individual lipid effects or due to the general order state of the membrane microenvironment. The microviscosity of the membrane is considered the main mechanism which modulates membrane protein function, although the possibility of extra effects of the Cho molecule cannot be discarded [2–4]. Moreover, the presence of CRAC motifs (Cho recognition/interaction amino acid consensus sequence) in G-protein coupled receptors has been identified [5]. For instance, the presence of binding sites has been postulated not only for fatty acids but also for sterols, in the lipid–protein interface of the acetylcholine receptor [6, 7].

There are several intrinsic membrane proteins modulated by the Cho content of membranes, such as the Serotonin 1A receptor [8, 9], GABA carriers [3], the brain oxytocin and cholecystokinin receptors [4, 10] and the acetylcholine receptor [7, 11]. In the particular case of the $GABA_A$ receptor ($GABA_A$-R), electrophysiological experiments showed that the membrane Cho content affected the coupling between the binding sites for Benzodiazepines and other drugs that interact with the receptor [12]. On the other hand, in radioligand-binding experiments, it was observed that this effect depended on the membrane source (brain, spinal cord, or cerebellum) and was related to the differential subunit composition of the receptor [13].

There are different methods to modify the Cho content of natural membranes, e.g., using lipid transfer-proteins that transport lipids in a non-specific way [3], incubating membranes with liposomes formed by a 1:1 lipid:Cho mixture [13], or using β-cyclodextrins (β-CD) or their substituted derivatives [14–16]. β-CDs are cyclic oligosaccharides obtained from the bacterial degradation of starch and consist of 7 glucose residues linked by $1 \longrightarrow \alpha 4$ glycosidic bonds. Their annular structure presents a non-polar, cylindrical cavity that binds and, therefore, solubilizes a great variety of hydrophobic molecules. This property enables its use as a drug vehicle and Cho linker [17–20]. β-CDs can be used to deplete or to enrich membranes with Cho, when they are incorporated into the membrane system alone or complexed with Cho, respectively. In addition to Cho and other lipids [21], the β-CD may also interact with proteins and peptides. As an example, it has been observed that β-CD interacts with a synthetic β-amyloid peptide of 40 amino acids, possibly through the aromatic residues of the peptide [22].

The activity of $GABA_A$-R has been tested in electrophysiological experiments in the presence of β-CD (0.5 mM) and GABA [23]. In studies on Cho-depleted brain membranes, alterations in the $GABA_A$-R surface density [24] have been reported. Moreover, correlations between membrane organization and $GABA_A$-R function have been proposed [25] but, to our knowledge, these have never been submitted to experimental demonstration. Likewise, possible β-CD–ligand interactions have never been considered.

In this study, we study the effects of β-CD treatment on Cho content and $GABA_A$-R activity in synaptosomal membranes (SM) purified from bovine brain cortex.

The organization of the SM was analyzed by electron paramagnetic resonance (EPR) spectroscopy, steady-state fluorescence anisotropy, and through Langmuir films of native, thermally treated and Cho-depleted membranes. On the other hand, [^{3}H]-Flunitrazepam (FNZ) was used to evaluate $GABA_A$-R ligand-binding activity. Careful was taken to assured the absence of possible artifacts induced by β-CD on Cho and protein quantitation and the possible formation of a [^{3}H]-FNZ–β-CD complex was evaluated. Finally, the effect induced by the thermal cycling accompanying the treatment with β-CD on the organization of the SM was also studied.

Methods

Materials

The Benzodiazepine diazepam (DZ) [26] was kindly supplied by Productos La Roche (Córdoba, Argentina).

[^{3}H]-FNZ was purchased from New England Nuclear Chemistry (E.I. DuPont de Nemours & Co. Inc., Boston, MA, USA). Doxyl stearic acids carrying the *N*-oxyl oxazolidine moiety at carbons 5 and 12, 1,6-diphenyl-1, 3,5-hexatriene (DPH) and 1-(4-trimethylammoniumphenyl)-6-phenyl-1,3,5-hexatriene *p*-toluenesulfonate (TMA-DPH) were obtained from Sigma Chemical Co., St. Louis, MO, USA. Other drugs and solvents were of analytical grade.

Natural Membrane Preparations

SM were obtained from bovine brain cerebral cortex. Meninges were eliminated, the cortex dissected and SM were purified essentially according to the method of Enna and Snyder, modified by Perillo and Arce [27], immediately lyophilized and stored at −20°C. This allowed the performance of all the experiments with an identical membrane source. Afterward, it was checked that similar results could be obtained with fresh membranes. SM were resuspended in 50 mM Tris–HCl buffer (pH 7.4) containing 100 mM NaCl at a final protein concentration between 0.047 and 0.25 mg/ml, depending on the experiment.

Treatment with β-CDs (Cho Depletion)

Bovine SMs were depleted of Cho using β-CD by applying typical procedures [9, 10, 14, 28]. In brief, 4 ml of SM (4 mg protein/ml) were treated with β-CD at a final concentration of 40 mM and incubated at 37°C for 30 min with periodic shaking. The membrane suspension was centrifuged at 18,400×*g* for 15 min and then resuspended in the same volume of 50 mM Tris–HCl buffer pH 7.4, 100 mM NaCl. This washing procedure was repeated twice to eliminate the β-CD from the system (CD-PI sample). The final pellet was resuspended in the same buffer at a final protein concentration of 0.25 mg/ml for binding and monolayer experiments, 0.047 mg protein/ml for fluorescence experiments, and 6–12 mg/ml for EPR experiments. Cho content was estimated using an enzymatic assay kit (Wiener Colestat, Rosario, Argentina). The control sample used to evaluate the effect of the pre-incubation (PI) consisted of SM pre-incubated at 37°C and submitted to the centrifugation process but in absence of β-CD (CON-PI sample). Control samples (CON) were not submitted to any physical (PI) or chemical (β-CD) treatment.

Binding of [^{3}H]-FNZ to Bovine SM

All the procedures were carried out at 4°C. The membrane receptor preparation was obtained as described above. The incubation system contained, in a final volume of 230 µl, the membrane suspension at a final protein concentration of 0.25 mg/ml, [^{3}H]-FNZ within a final concentration range of 0–12 nM (minimum specific activity 74.1 Ci/mmol), 100 mM NaCl–50 mM Tris–HCl buffer pH 7.4 containing (non-specific sample) or not (total sample) 9.4 µM DZ (final concentration). Samples were incubated at 4°C in the dark for 1 h and then filtered through SS filters (Whatman GF/B type) with an automatic harvester apparatus. The rinsed and air-dried filters were placed in vials containing 2.5 ml of scintillation liquid (25%V/V Triton X-100, 0.3% W/V diphenyloxazole in toluene). The retained radioactivity was determined with a Rackbeta 1214 scintillation counter (Pharmacia-LKB, Finland) with an efficiency of 60% for Tritium. Protein concentration was determined by the Lowry method [29].

The specific binding of [^{3}H]-FNZ was calculated as the total binding (measured in the absence of DZ) minus the non-specific binding (in the presence of DZ). Equation 1 was fitted to the saturation curves (specifically bound vs. free [^{3}H]-FNZ concentration), by a non-linear regression analysis performed by a computer-aided least squares method [30]:

$$B = \frac{B_{\max} F}{K_d + F} \quad (1)$$

where *F is* the free [^{3}H]-FNZ concentration, *B* and $B_{\max}$ are the ligand concentration-dependent and the maximal-specific binding activities, respectively, and K_d is the equilibrium dissociation constant.

EPR Spectra

EPR spectra were recorded at room temperature (22 ± 2°C) using a Bruker ER-200 SRC spectrometer operating at 9 GHz, and 0.2 ml flat quartz cells from Wilmad, Lab Glass (Buena, NJ). Spin labels (10^{-4} M) were incorporated into SM from films of the probes by vortexing for 2 min every 1 min, for a total time of 15 min. Phospholipid concentration was 10 mM in experiments using 5-doxylstearic acid spin label (5-SASL) and 20 mM in experiments using 12-doxylstearic acid spin label (12-SASL).

It is known that the pK of 5-SASL in natural membranes is 6.6 [31–33]. To insure that in our experimental conditions (pH 7.4), there were no splitting in the spectra that could be associated with the coexistence of two probe species derived from the acid–base equilibrium of the probe, spectra were also recorded from samples dispersed in pH 9.5 borate buffer. Results obtained were similar to those at pH 7.4 (not shown).

The spectral analysis of mobile spectra such as those of 12-SASL can be performed by measuring the ratio of low to central-field heights of the nitroxide resonances (h_{+1}/h_0, Fig. 1a), and in the case of more immobilized spectra such

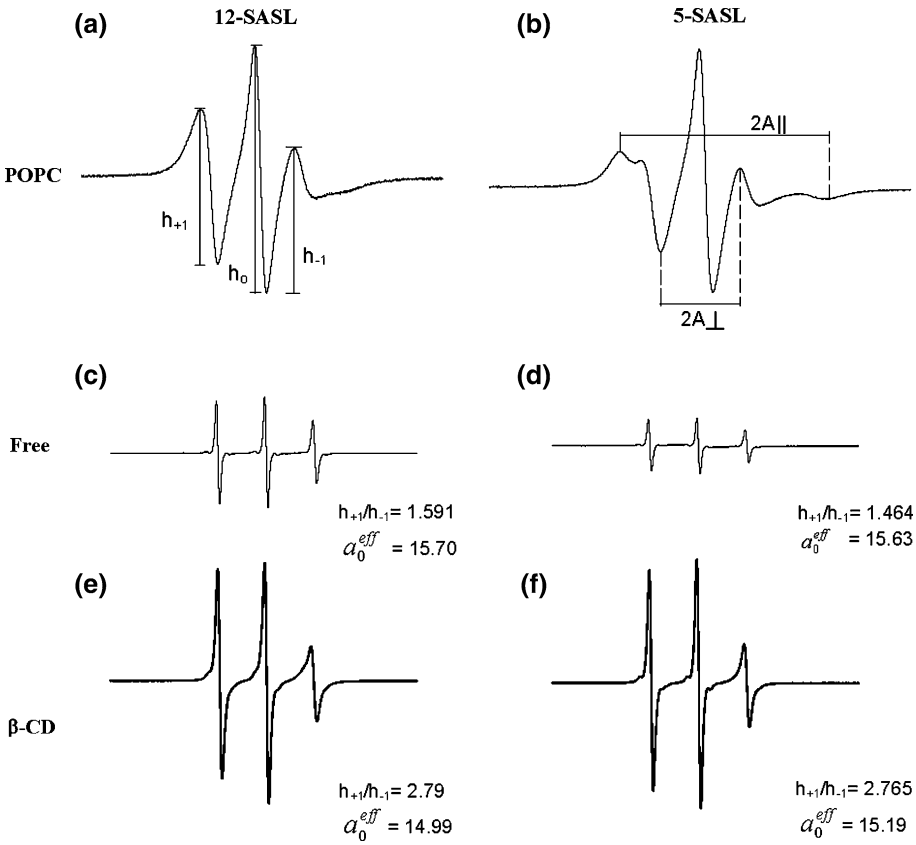

Fig. 1 EPR spectra of 12-SASL (**a**, **c**, **e**) and 5-SASL (**b**, **d**, **f**) incorporated in multilamellar phospholipid vesicles (1-palmitoyl-2-oleoyl-sn-glycero-3-phosphocholine) (**a**, **b**), in water dispersion (**c**, **d**) and complexed with β-CD (**e**, **f**). In these experiments, β-CD was assayed at a 5 mM final concentration (0.02 spin probe/β-CD molar ratio). h_{+1}/h_{-1} in the absence of SM (**c**–**f**) correspond to $h_{+1,\mathrm{MF}}/h_{-1,\mathrm{MF}}$

as those of 5-SASL, by calculating the order parameter S (Eq. 2).

$$S = \frac{A_{\|} - A_{\perp}}{A_{zz} - (A_{xx} + A_{yy})/2} \tag{2}$$

where $A_{\|}$ and $A_{\perp}$ are the outer and inner extrema, respectively, measured in the 5-SASL spectra (Fig. 1b) and A_{zz}, A_{xx}, and A_{yy} are the values of the principal components of the hyperfine coupling tensor (32.9, 5.9, and 5.4 Gauss, respectively) [34]. The measurement of h_{+1}, h_{-1}, and h_0 (height of the low, high, and central-field peak heights, respectively) in the spectra of 12-SASL is indicated Fig. 1a.

Each probe is able to sense at the depth where the labeled moiety is inserted within the bilayer. An increase in S implies a stiffening and lower flexibility of the acyl chain (i.e., increase order) due to a reduction of the *trans*-gauche isomerizations and the same is true for a decrease in the empirical parameter h_{+1}/h_0, which includes the contribution of both orientation and mobility [35].

In some cases, when the central-field peak signal of the membrane-incorporated probe was superimposed on the free probe signal (e.g., peaks pointed to by the arrows in Fig. 6c, f), the contribution of the free probe was evaluated through the parameter $h_{+1,\mathrm{MF}}/h_{-1,\mathrm{MF}}$ calculated as h_{+1}/h_0 but from spectra obtained either in the absence of SM (Fig. 1c–f) or from the component of probe not partitioned in the SM bilayers appearing in spectra of Fig. 6a–c, f. If compared with the behavior of 12-SASL and 5-SASL dispersed in water (Fig. 1c, d), the interaction of spin labels with β-CD was characterized by a broadening of the spectral lines (Fig. 1e, f). Because h_{+1} and h_{-1} were resolved satisfactorily in the presence of SM, there was no need of applying spectral substraction and the parameter $h_{+1,\mathrm{MF}}/h_{-1,\mathrm{MF}}$ could be calculated directly from the ratio of the height of the peaks.

The polarity of the environment sensed by the probes was estimated by the measurement of the isotropic hyperfine splitting (a_0^{eff}). These values were calculated for 5-SASL and 12-SASL in water and in the presence of β-CD. The spectra were recorded as a function of temperature (see Supplementary text) and a_0^{eff} was measured in conditions of high isotropic motion to insure that the parameter reflect only the contribution of the environment polarity. The corresponding EPR spectra were highly isotropic, hence a_0^{eff} values were obtained from the baseline-crossing points of the first-derivative spectra, otherwise Eq. 3 was used [36].

$$a_0^{\mathrm{eff}} = (1/3)(A_{\|} + 2A_{\perp}) \tag{3}$$

UV and Fluorescence Measurements

UV Absorbance Spectroscopy of FNZ

FNZ was dissolved in dioxane (between 0 and 82% V/V) aqueous solutions or in water containing or not β-CD at different FNZ:β-CD molar ratios (1:10, 1:20, 1:40). Absorbance spectra of FNZ in each solution were recorded with a Beckman DU 7500 (Fullerton, CA, USA) spectrophotometer equipped with a diode array detector and a sensitivity of 0.0001 AU.

DPH Fluorescence Spectroscopy

The fluorescence emission of DPH (4.8 μM) incorporated in the SM (0.047 mg protein/ml) was recorded at 430 nm (exciting at 356 nm) with a Fluoromax Spex-3 Jovin Yvon (Horiba, NJ, USA) spectrofluorimeter, equipped with a thermostated cell holder, a Xenon arc lamp, a photomultiplier tube as a signal detector and a photon-counting module. Excitation and emission slit widths were set at 2 nm. The membrane concentration was chosen so that the absorbance of the suspension was <0.1 [37].

Quantitative Spectral Analysis

To facilitate comparisons, the center of spectral mass (CSM) was calculated for each of the FNZ absorbance spectra and the DPH fluorescence emission spectra [38, 39] according to Eq. 4, where I_i is the absorbance or the fluorescence intensity (FI) measure at the wavelength λ_i.

$$\lambda = \frac{\sum \lambda_i \cdot I_i}{\sum I_i} \tag{4}$$

For non-symmetric spectra, CMS results a descriptor more appropriate than the value of λ at the maximal absorbance (λ_{max}). Changes in CMS would reflect modifications in the dielectric constant of the probe molecular environment mainly due to different accessibility to the solvent. In this study, this was applied: (a) in the case of FNZ, to demonstrate the ability of this $GABA_A$ ligand to partition inside the β-CD core, (b) in the case of DPH, to evaluate changes in the organization within the core region of SM upon PI treatment.

Calculation of Fluorescence Anisotropy

The fluorescence anisotropy of DPH (4 μM) and TMA-DPH (4 μM) was used to evaluate the effect of the PI treatment included in the protocol for Cho extraction using β-CD. FI was determined with the excitation and sample polarizer filters oriented parallel and perpendicular to each other. Steady-state fluorescence anisotropy was calculated according to Eqs. 5 and 6:

$$A = \frac{I_{VV} - I_{VH} \cdot G}{I_{VV} + 2 \cdot I_{VH} \cdot G} \tag{5}$$

$$G = \frac{I_{HV}}{I_{HH}} \tag{6}$$

where I_{VV}, I_{HH}, I_{VH}, and I_{HV} are the values of the different measurements of FI taken with both polarizers in the vertical (VV) or in the horizontal (HH) orientation or with the excitation polarizer vertical and the emission polarizer horizontal (VH) or vice versa (HV). G is a correction factor for differences in sensitivity of the detection system for the vertically and the horizontally polarized light [40].

Monolayer Studies

Monolayer experiments were performed at room temperature. The Teflon trough had a 24,075 mm^2 total surface area and contained 230-ml volume of bidistilled water used as a subphase. SM monolayers were formed by spreading an aqueous suspension (0.25 mg protein/ml) of SM on the air–water interface using a glass rod [41]. The surface pressure (π) (Wilhelmy method via platinized-Pt plate) and the area enclosing the monolayer (A) were automatically measured with a Minitrough II (KSV, Finland). The compression isotherm (π–A) was recorded continuously at a compression rate of 5 mm/min and the compressional modulus, K, was calculated according to Eq. 7.

$$K = -(A_\pi) \cdot \left(\frac{\delta\pi}{\delta A}\right)_\pi \tag{7}$$

Original SM vesicles actually acquired the monomolecular layer organization after they were spread at the air–water interface. This was shown by atomic force microscopy images (see Fig. 1S, Supplementary text) of the Langmuir–Blodgett (LB) films obtained by the transfer of monolayers from the air–water interface to alkylated glasses at a constant surface pressure of 35 mN/m. However, the possibility that some vesicles from the original SM material may have remained intact cannot be excluded. Although this would have affected molecular area value determinations, it would not have affected other qualitative conclusions that could be drawn from this membrane model. It is important to note that there is experimental evidence supporting the fact that LB films so obtained conserve the molecular organization of the original floating monolayer [42].

Statistical Analysis

Data were statistically analyzed using a two-tailed Student's t test for independent samples or a one-way analysis of variance (ANOVA), according to the experiment [43].

The values shown represent the mean and the standard error of the mean (SEM) of triplicate determinations. Linear regression analysis was performed by the least squares method.

Results and Discussion

Effect of the Treatment with β-CD on [^{3}H]-FNZ Binding to the GABA$_A$-R

Ligand-Binding Kinetic Parameters Analysis

The effect of β-CD treatment on GABA$_A$-R activity was evaluated by means of [^{3}H]-FNZ binding measurements. Saturation curves are shown in Fig. 2a. Non-specific binding curves showed a linear behavior and no significant differences were observed between the slopes of the samples tested (CD-PI, CON-PI, and CON). Specific binding curves showed a hyperbolic behavior reaching saturation. Figure 2b shows the binding parameters (K_d and B_{max}) determined from non-linear regression analysis of the saturation curves in Fig. 2a. The PI (CON-PI) and, although at a lower extent, also the β-CD treatment (CD-PI) induced an increase in the B_{max} values with respect to $B_{max,CON}$. Moreover, $B_{max,CD-PI}$ and $B_{max,CON-PI}$ were also significantly different from each another. This effect of the PI at 37°C had already been observed in fresh (not lyophilized) chick brain SM pre-incubated at 25°C [25]. The CD-PI showed a significant decrease in B_{max} compared with CON-PI. $K_{d,CON-PI}$ and $K_{d,CD-PI}$ were not significantly different from one another but showed an increase (statistically significant) with respect to $K_{d,CON}$, which indicated that β-CD treatment itself did not affect the affinity of the FNZ binding site although the accompanying thermal annealing did.

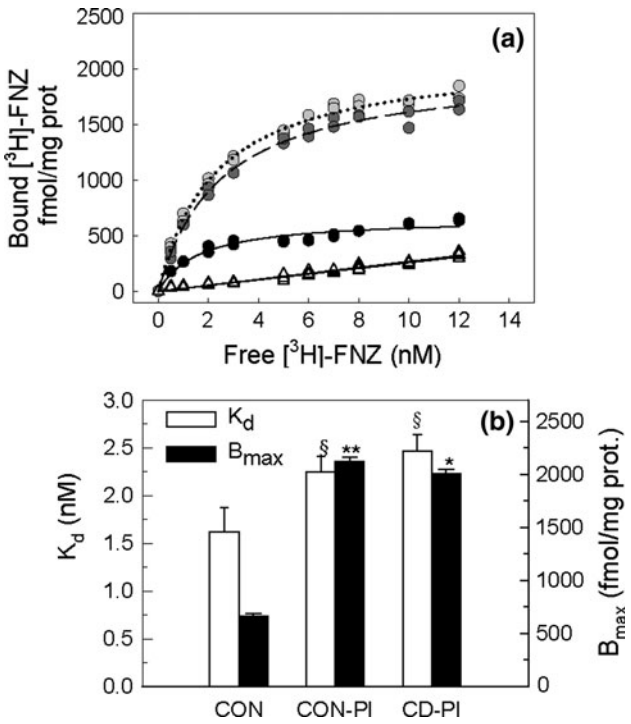

Fig. 2 Effect of β-CD on [^{3}H]-FNZ binding to SM. **a** Saturation curves. Specific (*filled circle*) and non-specific (*open triangle*) [^{3}H]-FNZ binding. *Full lines* CON, *dotted lines* CON-PI, and *dashed line* CD-PI. **b** Kinetic parameters determined from the non-linear regression analysis of curves depicted in (**a**). Values correspond to the mean ± SEM of duplicates. **Statistically different from the CON (Student's *t* test $p < 0.05$). *Statistically different from CON-PI (Student's *t* test $p < 0.05$). §Statistically different from the CON (Student's *t* test $p < 0.005$)

The inhibitory effect of β-CD observed on the binding of [^{3}H]-FNZ may be actual or artifactual depending on the underlying mechanism/s, which may be one or a combination of the followings:

a) An interference of β-CD in the Lowry method leading to an overestimation of the protein concentration and therefore to an underestimation of the B_{max} value, or "*vice versa*".
b) A direct interaction of remanent β-CD: (1) with the ligand (FNZ), by inducing an overestimation of the non-specific binding; (2) with the GABA$_A$-R, by affecting the ligand-binding affinity or capacity; (3) with the membrane, by incorporating in it and inducing subsequent structural changes.
c) The expected change in the membrane composition (Cho depletion), with the consequent effects on membrane organization.

Hypotheses a–c were evaluated as follows:

β-CD does not Interfere in Cho and Protein Quantitation (Hypothesis a)

The presence of a residual amount of β-CD that might not have been eliminated by the centrifugation process could have interfered with the chemical methods used to analyze the composition of SM. To discard possible artifacts, the concentration of standard solutions of Cho (Fig. 3a) and bovine serum albumin [44] (Fig. 3b) were determined in the presence of increasing concentrations of β-CD. Assuming that in a typical experiment β-CD would be retained in a 0.1-ml volume pellet, and considering the 40 mM β-CD concentration of the stock solution used for Cho depletion, it was possible to estimate that the maximum final concentration of β-CD that could be found in the SM suspension after two cycles of washing by centrifugation and resuspension in the initial volume of buffer (see "Treatment with β-CDs (Cho depletion)" section) would

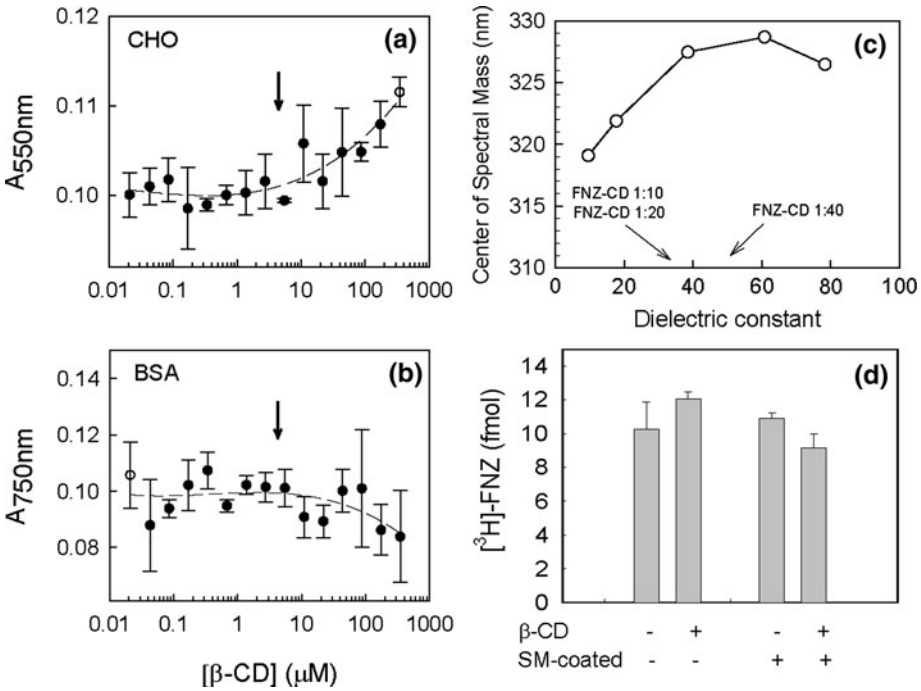

Fig. 3 Possible artifacts in the [^{3}H]-FNZ binding assay. Effects of the β-CD concentration on the Cho (**a**) and protein (**b**) quantitation in standard solutions of Cho (0.009 g/ml) and BSA (0.1 mg/ml). *Arrows* point to the estimated residual β-CD concentration in Cho-depleted SM samples. **c** Complexation of FNZ with β-CD evaluated through the effect on FNZ absorbance spectra. The CSM values were calculated between 290 and 400 nm from absorbance UV spectra of FNZ in solutions of known dielectric constants or in β-CD aqueous suspensions at the indicated FNZ-β-CD molar ratios. Interpolating (*dotted lines*) the latter in the CSM-D plots showed that, in the presence of β-CD, FNZ is located in an environment less polar than water. **d** Non-specific retention of [^{3}H]-FNZ on the glass filters. 10 µl of a 115 nM [^{3}H]-FNZ solution containing (+) or not containing (−) 40 mM β-CD was filtered through Whatman GF/B glass filters. Previously, 230 µl of either a SM suspension (0.25 mg protein/ml) or water had been passed through the same filters to obtain the SM-coated (+) and the clean (−) filters, respectively

be approximately 25 µM, 1,600 times smaller than the initial β-CD concentration. In both kinetics and monolayer experiments, the SM was 16 times more diluted than in other experiments (this can be calculated by considering the protein concentration in the initial SM suspension obtained after the two washing steps (4 mg/ml) and that of the SM suspension used in binding and monolayer experiments (0.25 mg/ml)). Then, the final β-CD concentration would be 1.5 µM. Both concentrations are within the β-CD concentration range at which β-CD, according to the results shown in Fig. 3a, b, does not interfere with the quantification of either Cho or proteins. On the other hand, in the SM suspension used for EPR analysis, the concentration of β-CD remaining can be estimated as 37–75 µM, taking into account that the final pellet was less diluted than for other experiments (see "Treatment with β-CDs (Cho depletion)" section).

β-CD does not Affect the Non-specific Binding of [^{3}H]-FNZ to SM (Hypothesis b1)

The FNZ–β-CD interaction was investigated by UV spectroscopy (Fig. 3c). FNZ absorbance spectra showed an increase in CSM as a function of the medium polarity (identified by its dielectric constant value). Then, the interpolation of the CSM determined in aqueous suspensions of β-CD showed D values lower than the corresponding $D_{water} = 82$ at 21°C. This indicated that FNZ was located in an environment with a polarity lower than that expected for the free drug in water and supported the FNZ–β-CD complex formation. Hence, this result suggested that, during the binding protocol, the entrapment of [^{3}H]-FNZ inside the hydrophobic core of the β-CD molecules remaining in SMs after the Cho depletion procedure could have caused an increase in [^{3}H]-FNZ non-specific binding, leading to an artifactually reduced specific binding. However, as stated above, the amount of β-CD remaining after the three washings applied in the Cho depletion procedure was too small to induce a detectable effect. Moreover, if the sequestration of [^{3}H]-FNZ inside the β-CD hydrophobic core was significant, it would have led to a decrease in free [^{3}H]-FNZ concentration detectable by an apparent increase in the K_d values, which was not observed.

On the other hand, the non-specific retention of [^{3}H]-FNZ in the glass filters during the fast filtration process (Fig. 3d) was not favored by the presence of β-CD since

similar results were obtained either using clean filters or with SM pre-coated filters. In addition, the slopes of non-specific binding curves coming from samples with or without β-CD were indistinguishable from each other (24.54 ± 0.22 fmol/mg protein/nM) (Fig. 2a).

Taken together, these results confirmed that the specific binding determinations produced reliable values that allowed them to be analyzed in terms of ligand–receptor interactions. It is possible that lipid–protein interactions were responsible for maintaining the activity of $GABA_A$-R, and the lack of Cho after β-CD treatment could have resulted in a reduction in $B_{max,CD\text{-}PI}$ compared with $B_{max,CON\text{-}PI}$ value.

$GABA_A$-R–β-CD Interaction (Hypothesis b2)

The decrease in B_{max} could have been due to the direct interaction of β-CD with the receptor protein (non-competitive inhibition). In that case, the β-CD–$GABA_A$-R interaction might have induced a change in the protein conformation, preventing FNZ binding. Although electrophysiological experiments suggested an effect of β-CD on the $GABA_A$-R conformation [19], this effect was observed in the presence of β-CD at a concentration (0.5 mM) significantly higher than what we estimated as remaining in our samples (1.5 μM; see "Surface pressure–area compression isotherms" section).

Another mechanism of direct action of β-CD on the [^{3}H]-FNZ binding could have been its direct interaction with the FNZ binding site at the receptor but, in that case, changes in the affinity binding of [^{3}H]-FNZ should have been observed, which did not happen.

β-CD–Membrane Interaction (Hypothesis b3)

In Fig. 4, the EPR spectra of the spin probe 5-SASL recovered in the supernatant obtained after the centrifugation washing process of CD-PI and CON-PI samples are shown. The supernatant of CD-PI samples exhibited spectra with $h_{+1}/h_{-1} = 2.874$ (Fig. 4a), very similar to that of the β-CD–probe complex (Fig. 1f). On the other hand, supernatants of CON-PI samples exhibited 5-SASL EPR spectra characteristic of an immobilized probe in an anisotropic environment (Fig. 4b) (with an order parameter of $S \sim 0.779$). This indicated that in CON-PI samples a fraction of membrane did not have precipitated. This was not observed in CD-PI samples, suggesting that β-CD favored membrane sedimentation upon centrifugation. Although this could be explained by the change in membrane Cho content (see below), which was the expected effect, the very small amount of the remaining β-CD could have also contributed somehow to modify some physical properties of the membranes leading to the increased

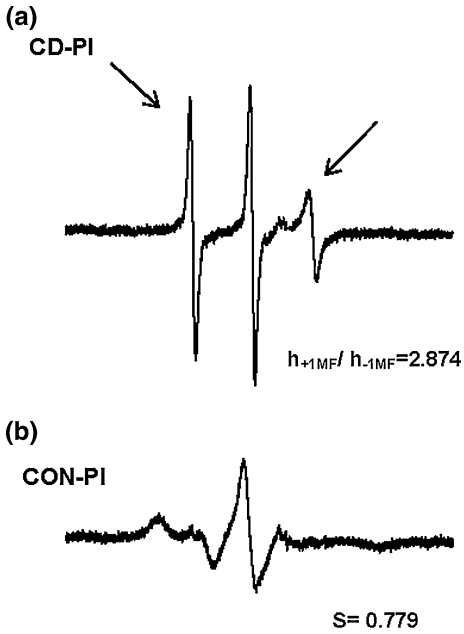

Fig. 4 EPR spectra of 5-SASL in the supernatants of CD-PI (**a**) and CON-PI (**b**) samples, obtained after the third wash. Spectra are the result of the accumulation of four scans. The lower intensity of the signal in (**b**) was due to the small amount of membrane remaining unpelleted

compactness of the pellet obtained, since the β-CD interaction with membrane components [45] as well as the formation of complex that imply β-CD molecules bound to external vesicles surfaces have already been described [46].

Effect of β-CD on Membrane Composition (Hypothesis c)

The total phospholipids, Cho, and protein composition of all the SM sample types used are shown in Table 1. The chemical composition of the untreated bovine SM (CON) was similar to that determined previously by other authors [47]. The composition of CON-PI was not statistically different from that of CON at a significance level of 5%, whereas in CD-PI a significant decrease in phospholipids and Cho content was observed with respect to CON. Consequently, it is possible to affirm that the Cho depletion was successful and that it was accompanied by other changes in chemical composition, such as in phospholipids, in agreement with previous reports [45, 48]. The apparently greater protein concentration in CD-PI with respect to CON and CON-PI (Table 1) should be ascribed to a β-CD-induced improvement of the membrane recovery, during the centrifugation process explained above. Consequently, the Cho content of β-CD-treated membranes evaluated in terms relative to the protein concentration resulted as approximately 45% of the initial value. β-CD-induced changes in membrane composition affected membrane organization, which will be considered in a separate section.

Table 1 Effect of β-CD on the chemical composition of bovine SM

Samples	Phosph/SM (mg/mg)	Cho/SM (mg/mg)	Protein/SM (mg/mg)	Cho/protein (mg/mg)
CON	0.300 ± 0.008	0.103 ± 0.003	0.264 ± 0.008	0.389 ± 0.023
CON-PI	0.267 ± 0.025	0.093 ± 0.004	0.256 ± 0.002	0.363 ± 0.018
CD-PI	0.205 ± 0.015[¶]	0.050 ± 0.010[§¶]	0.316 ± 0.010[§]	0.158 ± 0.037*[¶]

SM synaptosomal membranes, *CON* SM neither pre-incubated nor centrifuged, *CON-PI* SM pre-incubated and centrifuged but in absence of β-CD, *CD-PI* SM submitted to β-CD treatment, *Phosph* phospholipid, *SM* synaptosomal membranes used as starting material. Values correspond to the mean ± SEM (3)

*,§ Statistically different from the CON-PI with $p < 0.001$ or $p < 0.05$, respectively (one-way ANOVA)

¶ Statistically different from the CON (one-way ANOVA), $p < 0.001$)

β-CD Effect on SM Organization

To test the composition-dependent organization of SM, three approaches were applied: (a) isothermal compression of monomolecular layers, (b) EPR spectroscopy using 5-SASL and 12-SASL as probes, and (c) steady-state fluorescence spectroscopy of DPH and TMA-DPH.

Surface Pressure–Area Compression Isotherms

β-CD-treated SM were characterized according to their behavior at the air–water interface by means of π–area compression isotherms of CON, CON-PI, and CD-PI samples (Fig. 5a). The π–area isotherms of CON-PI monolayers were less expanded and the typical phase transition, usually associated with protein reorganization at the surface [49], was less evident than in CON. The isotherm of CD-PI exhibited a compressibility even slightly lower than CON-PI and lacked a phase transition. The compression modulus-area isotherms were calculated from π–*A* data (Fig. 5b). The PI induced an increase in the value of *K* calculated at a π near the equilibrium pressure of bilayers (see interpolation in Fig. 5b). Taking the CON sample as a reference, the analysis of π–*A* and *K*–*A* isotherms suggested that the most significant change in monolayer structure was associated with PI treatment of the SM. The latter could be related to a higher head group hydration in the thermally annealed (PI) samples, if compared with CON, which led to an easier molecular spread over the air–water interface and different general organization, resulting in a net increase in molecular packing. The effect of β-CD treatment on isotherm compressibility was opposite to that expected from the mere Cho loss (it should have produced an even more expanded monolayer than that of the CON) thus reflecting the complex change in the chemical composition of SM (Table 1). The behavior of highly packed monolayers could be extrapolated to denser bilayers [50] and this would explain the greater efficiency in the precipitation of SM in CD-PI samples upon centrifugation (Fig. 4a). It is important to note that the incorporation of

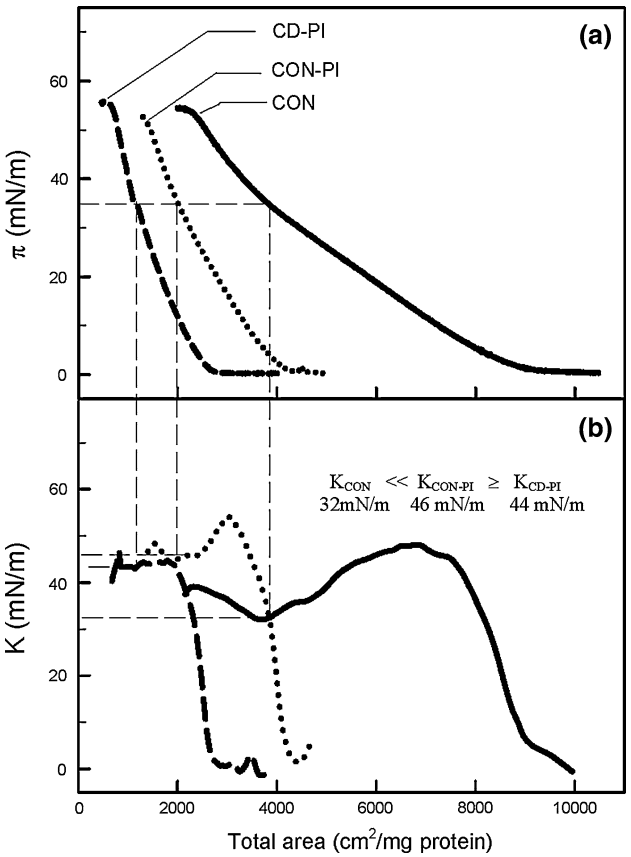

Fig. 5 Effect of PI at 37°C with or without β-CD on the π–A compression isotherms (**a**) and compressional modulus (*K*) (**b**) of monolayers obtained through the spreading of SM at the air–water interface. *CON* non-treated, *CON-PI* pre-incubated at 37°C and centrifuged, *CD-PI* treated with 40 mM β-CD. *Dashed lines* indicate the interpolations performed to determine *K* values at $\pi = 35$ mN/m which is near the equilibrium π of bilayers

β-CD to a lipid monolayer from the subphase induced a surface pressure increase (Fraceto and Perillo, unpublished data), which can be rationalized as higher molecular packing. This may explain the direct influence of the remaining small amounts of β-CD on the CD-PI samples of SM preparation.

EPR Experiments

Figure 6 depicts EPR spectra of 12-SASL and 5-SASL incorporated in CON, CON-PI, and CD-PI samples. As shown in Fig. 6a–c, the spectra of 12-SASL exhibited two spectral components corresponding to two different membrane environments. One of them corresponded to the probe located next to protein molecules (immobilized component, I) and the other corresponded to the probe located in a more fluid lipid phase (mobile component, M). It is important to note that both M and I components are different from the highly mobile component corresponding to probe in the aqueous phase (free spin labels), which appears as a narrow peak, clearly seen in the h_{+1} and h_{-1} peaks of the EPR spectrum of 12-SASL (Fig. 6a, b).

Figure 6b also shows a PI-induced decrease in the relative contributions of I and M components. Since the total amount of 12-SASL present in the sample is constant, changes in the relative intensities of I and M spectral components could be understand as a change in the differential partition of 12-SASL between protein-rich (I) and lipid-rich (M) phases. PI might be improving the accessibility of 12-SASL to the protein-rich phase or a redistribution of protein and lipid components between phases.

The mobility parameter of 12-SASL (h_{+1}/h_0) contained three components: mobile, immobile, and free spin labels. Unfortunately, all of these components are present in the central line and affected the amplitude of the low- and high-field line. Due to this phenomena, conclusions based on mobility measurements would have been somewhat weakened hence, this kind of information from 12-SASL spectra could not be used to analyze the membrane organization in the inner membrane core. So, to obtain information about the membrane organization in the hydrocarbon chain region, a fluorescent anisotropy study with DPH probe was made (see below).

Nevertheless, based on the comparative analysis of $h_{+1,MF}/h_{-1,MF}$ value of CD-PI (2.73 ± 0.03) and the

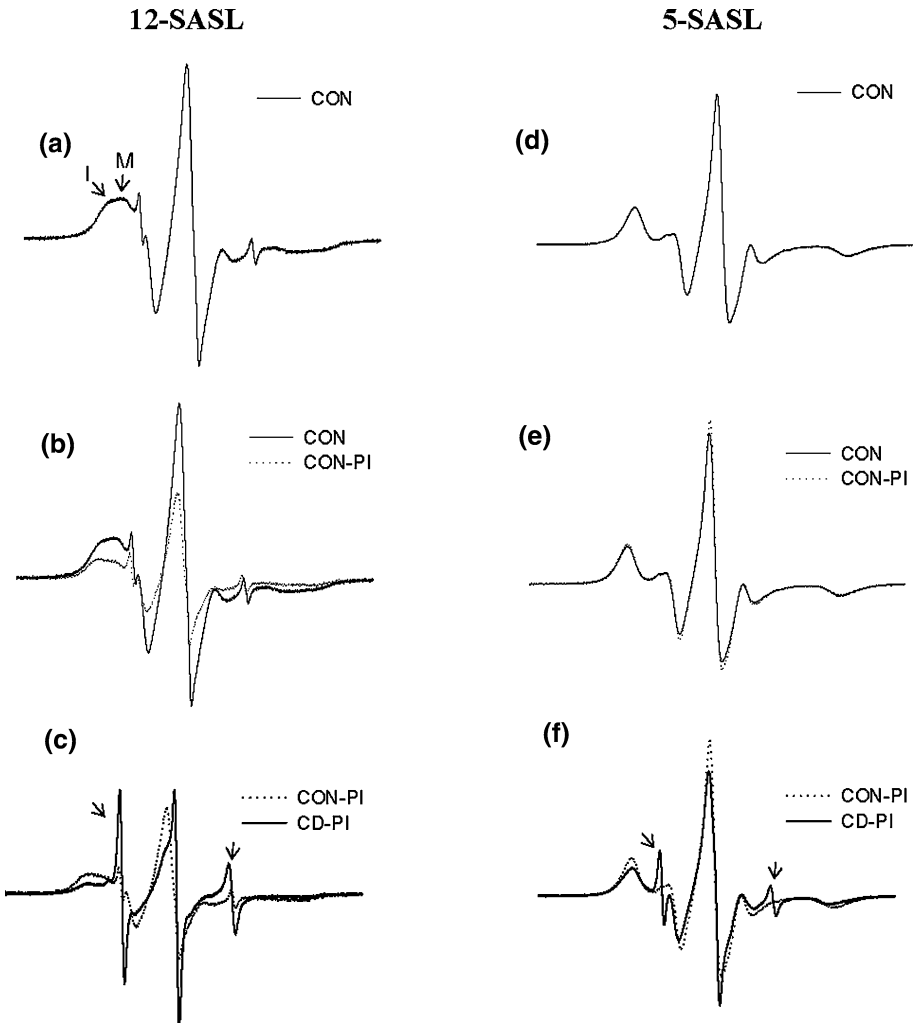

Fig. 6 EPR spectra of 12-SASL (**a**–**c**) and 5-SASL (**d**–**f**) incorporated in control SM (CON; **a**, **d**) as well as β-CD-treated (CD-PI; **c**, **f**) and non-treated (CON-PI; **b**, **e**) samples. In (**a**), I and M indicate the immobile and mobile spectral components, corresponding to probe interacting with proteins and lipids, respectively. In *central* and *lower panels*, spectra of CON-PI (**b**, **e**) and CD-PI (**c**, **f**) were superimposed with those of their corresponding control sample (CON and CON-PI, respectively) for comparison. In (**c**), it is shown that a fraction of probe molecules in the CD-PI sample was partitioned inside β-CD because the probe immobilized inside the membrane contributes to the whole spectrum with a lower intensity than in CON-PI (comparing the low field peaks of both superimposed spectra). In (**c**, **f**), *arrows* point to peaks corresponding to the spin label interacting with the β-CD that remains in the pellet. In these experiments, the β-CD/phospholipids molar ratio was 0.004

Table 2 Effect of β-CD treatment on SM as evaluated from 12-SASL and 5-SASL EPR and DPH fluorescence spectra

Treatment	12-SASL		5-SASL			DPH
	$h_{+1,MF}/h_{-1,MF}$	a_0^{eff} (G)	S	$h_{+1,MF}/h_{-1,MF}$	a_0^{eff} (G)	CSM (nm)
With SM						
CON	1.92 ± 0.04		0.77 ± 0.01	–		446
CON-PI	1.22 ± 0.58		0.76 ± 0.00	–		443
CD-PI	2.73 ± 0.03		0.72 ± 0.00 *	2.50 ± 0.01		nd
Without SM						
Water	1.64 ± 0.01	15.70	–	1.58 ± 0.00	15.63	–
CD	2.79 ± 0.00	14.99	–	2.77 ± 0.08	15.19	–

Parameters calculated from EPR spectra shown in Fig. 1c–f (without SM) and Fig. 6 were defined as follows: (a) $h_{+1,MF}/h_{-1,MF}$, calculated as a h_{+1}/h_{-1} but applied to the component of probe molecules not incorporated in the membrane bilayer (MF) but either dispersed in the aqueous fraction or partitioned inside β-CD; (b) a_0^{eff}, isotropic hyperfine splitting constant (obtained from the baseline-crossing points of the corresponding first-derivative spectra); (c) S, order parameter measured on 5-SASL spectra (Fig. 6d–f) according to Eq. 2; (d) CSM of DPH fluorescence spectra calculated according to Eq. 3

* Statistically different from CON-PI (Student's t test $p < 0.05$). Values correspond to the mean ± SEM of triplicates

$h_{+1,MF}/h_{-1,MF}$ determined in membrane-free (MF) samples in the presence and in the absence of β-CD (2.79 ± 0.00 and 1.64 ± 0.01, respectively), the narrow peaks in the 12-SASL spectra obtained in CD-PI samples (Fig. 6c), could be assigned to probe molecules trapped inside the β-CD core (Table 2).

5-SASL spectra in CD-PI (Fig. 6f) also exhibited a component derived from the probe trapped in β-CD (see $h_{+1,MF}/h_{-1,MF}$ in Table 2). In spite of this, it was possible to calculate the order parameter, showing that $S_{CON\text{-}PI}$ was similar to S_{CON} while $S_{CD\text{-}PI}$ was significantly smaller than $S_{CON\text{-}PI}$ (Table 2). Hence, the molecular order in the region of the hydrocarbon chains close to the polar group (sensed by 5-SASL) was lower in CD-PI with respect to CON-PI. This was a clear indication that the decrease in Cho content induced a decrease of molecular order within this region of SM. Contrary to what was observed in the present work with β-CD-treated SMs, methyl-β-CD-treated red blood cells [51] exhibited an increase in the 5-SASL EPR order parameter accompanying the Cho depletion. This could be ascribed to the difference in the membrane source, to the different β-CD derivatives, or both.

It has been shown that the effective ^{14}N-hyperfine coupling constants (a_0^{eff}) of n-SASL spin labels in phospholipid membranes decreases as a function of n, and thus the nitroxide moiety was located more deeply in the membrane, in a less polar environment [36]. In water, a_0^{eff} for 12-SASL and 5-SASL displayed very similar values (15.70 and 15.63, respectively), while in the presence of β-CD a_0^{eff} for both spin probes decreased significantly with respect to those in water, with $a_{0,5\text{-SASL}}^{eff}$ in β-CD (15.19) being significantly higher than $a_{0,12\text{-SASL}}^{eff}$ 14.99). These results (summarized in Table 2) suggested that the spin probes were bound to β-CD through the carbohydrate chain, with their nitroxide moiety located close to the β-CD hydroxyl–water interface, an environment that appeared slightly less polar than bulk water but more polar than a membrane interior (Fig. 2S, in supplementary text). This would allow a deeper penetration, hence a stronger immobilization, of 12-SASL inside the β-CD core allowing the stabilization of its nitroxide moiety in a less polar environment compared with 5-SASL. This rationale is in accordance with a previously proposed model [52].

In brief, the EPR experiments also confirmed that: (a) PI did not affect the interfacial region (monitored by 5-SASL), which might be related to changes in the hydration of the lyophilized membrane after the thermal annealing induced by PI at 37°C; (b) the β-CD-induced Cho depletion reduced membrane order near the interfacial region (decrease in the 5-SASL order parameter S); (c) β-CD was able to bind both 5-SASL and 12-SASL (Fig. 1c, f) and β-CD–spin probe complexes could be retained in SM (Fig. 6c, f; Table 2).

Steady-State Fluorescence of DPH and TMA-DPH

The PI associated with β-CD treatment affected the binding of [^{3}H]-FNZ to SM. To test if this was an irreversible effect of temperature on the organization of the SM, the thermotropic behavior of SM was studied by the means of steady-state fluorescence spectroscopy of DPH and TMA-DPH (Fig. 7). In addition, DPH could supply the information about membrane organization within the core region not accessible with 12-SASL due to the high contribution of the non-bound signal which masked the partitioned component of the spin probe. Both probes localize at different depths within biomembranes. DPH, being a highly hydrophobic molecule, partitions within the

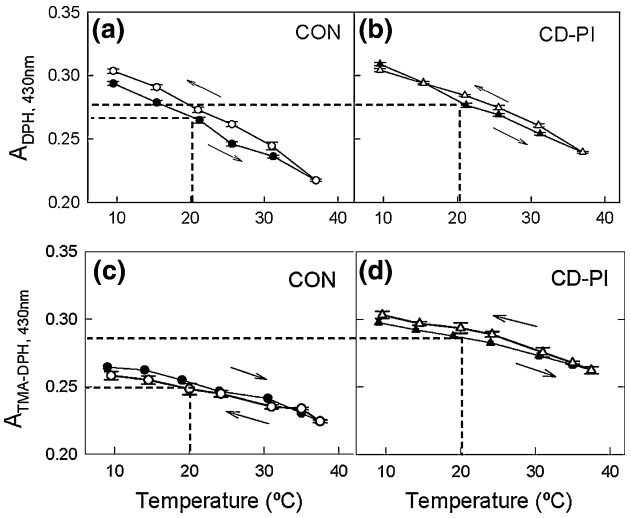

Fig. 7 Effect of temperature on DPH (**a**, **b**) and TMA-DPH (**c**, **d**) fluorescence anisotropy. CON and CD-PI samples were heated and cooled and the anisotropy values were measured within the cycle. *Arrows* point toward the direction of temperature change. *Dashed lines* in **a** and **b** highlight that anisotropy values at 20°C were higher for *β*-CD-treated SM compared with CON samples even after PI at 37°C. Note that lower right points in **a** and **c** (the point at 37°C in the heating CON curves using DPH and TMA-DPH, respectively) are equivalent the CON-PI sample. DPH and TMA-DPH concentrations were 4.8 μM. $\lambda_{ex} = 356$ nm, $\lambda_{em} = 430$ nm with both probes

hydrocarbon chain region of bilayers. On the other hand, TMA-DPH bears a net positive charge in its ammonium moiety that makes the molecule hydrophilic, becoming trapped with its DPH moiety at the polar head group region of membrane bilayers [53]. The anisotropy of the DPH fluorescence (A_{DPH}) enabled molecular membrane order to be assessed in the deepest membrane region. A_{DPH} diminished significantly with temperature in CON (Fig. 7a) as well as in CD-PI (Fig. 7b) samples, reflecting the decreasing rotational restrictions imposed by the surroundings on the molecular probe. $A_{TMA-DPH}$ (Fig. 7c, d) was lower (more significantly at the lowest temperatures) in CON than in CD-PI and less sensitive to temperature than A_{DPH}. The latter is consistent with data reported in the literature showing that the deeper hydrocarbon region of the hippocampal membrane is more sensitive to changes in membrane organization and dynamics due to Cho depletion than the interfacial region [8]. As expected, the cooling process followed a behavior opposite to that of heating, increasing A_{DPH} and $A_{TMA-DPH}$ as a function of temperature. However, only with DPH, the system exhibited hysteresis evidenced by the higher A_{DPH} values registered in the cooling direction compared with the heating. A parallel analysis of anisotropy and binding protocols showed that PI at 37°C irreversibly modified SM organization since, once cooled, the sample did not recover neither initial binding nor anisotropy values, which became significantly higher than before PI.

This is consistent with the higher compressional modulus K of monolayers derived from CON-PI compared with those from CON samples (Fig. 5b) as well as with the changes in the CSM of the fluorescence spectra of DPH partitioned in SM which were blue-shifted in CON-PI with respect to CON (Table 2), suggesting a lower polarity of the DPH environment possibly related to a decreased water accessibility derived from higher molecular packing.

In the final state after the 4–37–4°cycle, DPH was in a more ordered and hydrophobic atmosphere than in the initial state (the CSM diminished from 446 nm in CON to 443 nm in CON-PI, Table 2). This irreversible change in organization might be the cause of the irreversible change in kinetics parameters of [^{3}H]-FNZ binding in CON-PI with respect to CON (Fig. 2b). This quantitatively important increase in B_{max} values cannot be explained by a simple increase in the partition of [^{3}H]-FNZ because that effect would have been observed in the non-specific samples and discounted from the total binding when calculating the specific binding. On the contrary, the increase in $B_{max,CON-PI}$ could be explained by an increase in the recruitment or rearchitecturing of the binding sites. Moreover, our results suggest that hysteresis during the heating–cooling cycle may be characteristic of these complex membranes because similar behavior in B_{max} was observed with fresh (not lyophilized) SM from chick brain submitted to a thermal treatment similar to the PI applied in the present work [54].

The *β*-CD treatment induced an increase in both A_{DPH} and $A_{TMA-DPH}$ (higher in the latter). In agreement with our results, Mukherjee and Chattopadhyay [Fig. 8 in 55] showed that, below 40°C, Cho-depleted bovine hippocampal membranes exhibited a DPH fluorescence polarization higher than native membranes. Unfortunately, we were unable to contrast the increase in A_{DPH} with EPR experiments due to the superposition of membrane-incorporated and free 12-SASL spectra (Fig. 6c). On the other hand, the increase in $A_{TMA-DPH}$ was not only against the decrease in the anisotropy of TMA-DPH (an extrinsic fluorescence probe) reported recently in CD-treated CHO-K1/A5 cell [7] and of Nile red in bovine hippocampal membranes [56] but also against the decrease in the order parameter measure with 5-SASL (Table 2). This discrepancy may be ascribed to the fact that TMA-DPH fluorescence anisotropy reflects an average organizational landscape which might include a possible *β*-CD partitioning. On the contrary, from EPR spectra of 5-SASL it was possible to resolve contributions from the probe partitioning within different molecular environments demonstrating the decrease in membrane organization near its head group region (Fig. 5f; Table 2). Although it is expected a direct linear relationship between probe fluorescence anisotropy, membrane order, and Cho content, there is considerable

experimental evidence in the literature that supports a different viewpoint. So it is very interesting to note that, when contour plots of the anisotropies of Laurdan [57] and DPH [58] and the FIs of nystatin and prodan [59] were superimposed on the temperature–Cho content phase space, a non-linear dependence of anisotropy or FI versus Cho concentration could be seen, particularly at low temperatures [e.g., at 30°C it was possible to go from a liquid-ordered (Lo) phase at $x_{Cho} < 0.02$ to a solid ordered (So) at $0.02 < x_{Cho} < 0.22$ coming back to Lo phase at higher x_{Cho}]. When very small intervals in Cho molar fractions were tested, variations in a well defined pattern (oscillations) could be observed in the partition coefficients of nystatin [60] as a function of Cho content, which was ascribed to the existence of a sterol superlattice [61] stabilized at specific Cho proportions in the liposome. The hexagonal superlattice organization can hardly be expected in natural membranes, in view of the heterogeneity of their lipid composition, the presence of proteins, the transbilayer asymmetry of phospholipid species, and the interactions with the cytoskeleton. However, similarities between various types of liposomes and human erythrocytes treated with various concentrations of methyl-β-CD to remove defined amounts of Cho were observed in the pattern of A_{DPH} contour lines within a Cho/temperature phase map that covered a 24–48°C temperature range [58]. These pieces of evidence may be another explanation for the results depicted in Fig. 7 if we consider that the decrease in Cho content of SM after β-CD treatment could have shifted the membrane state toward a local high anisotropy island or strip within the temperature–Cho phase plane.

Moreover, we cannot exclude the possibility that additional lipids (Table 1) and also proteins [62] extracted in our experiments contributed to the results found for SM. In addition, probe immobilization inside β-CD trapped in the membrane might be contributing to the increase in A_{DPH} and $A_{TMA\text{-}DPH}$ in CD-PI compared with CON. This is supported by the increase in the anisotropy of DPH and TMA-DPH in aqueous solution in the absence or in the presence of β-CD (Table 1S, in supplementary text) and data from NMR spectroscopy [63].

Coupling Between Membrane Organization and $GABA_A$-R Activity

In summary, it is necessary to distinguish the effect of the PI from that of the Cho depletion.

Effects of PI Treatment

The PI treatment in addition to favor β-CD accesses to the membrane components affected membrane organization and function. Temperature cycling may involve a walk along a complex phase space and may exhibit several typical symptoms of irreversible behavior. This is related to the appearance of slow rearrangement modes during the phase transitions with characteristic times longer than experimental time scales and/or with the existence of long-lived non-equilibrium states in the biomembranes. Such slow relaxation phenomena may include the formation of phases which are metastable over the whole range of their existence, a slow formation of the nascent phase requiring isothermal annealing out of the transition region and different non-convergent transition pathways (hysteresis) in heating and cooling.

The first indication that PI might be affecting membrane properties within the receptor surroundings, was provided mainly by the increase in the B_{max} of [^{3}H]-FNZ to SM. The small decrease in the binding affinity also suggested that PI operated subtle changes in the conformation of the receptor protein at an extent capable of being sensed by the folding of binding site.

The physical state of the bulk membrane phase determines the extent and rate of its spreading as a monomolecular layer from the bulk bilayer phase when placed over the aqueous surface. This explains that monolayers from PI membranes were less liquid-expanded and lacked the typical bidimensional phase transition, suggesting a stronger molecular packing in the PI-treated bilayer. Moreover, DPH anisotropy experiments demonstrated that the change in the molecular organization induced by PI was irreversible. The decrease in molecular mobility within the surroundings of DPH can be explained by the temperature-induced changes in the hydration (thermal annealing) of the membrane surface that were transmitted to the membrane interior [64]. Consequently, the correct spanning of the bilayer by integral proteins after PI could contribute to the straightening of the acyl chains, leading to decreased fluidity in the hydrophobic core. This hypothesis is supported by the differential partitioning of 12-SASL within protein and lipid phases of SM (Fig. 6b) (Since the total amount of 12-SASL present in the sample is constant, changes in the relative contribution of I and M spectral components could be understand, as a change in the partition of 12-SASL between lipid-rich (M) and protein-rich (I) phases, PI might be improving the accessibility of 12-SASL to the protein-rich phase or a redistribution of protein and lipid components between phases). Moreover, these changes in the membrane spanning of integral proteins after PI would explain the recruitment of a pool of $GABA_A$-R (B_{max} increase), not accessible to the ligand molecules before the PI, shown in this article and reported previously with chick's SM [25]. It seems that PI does not induce effects on the molecular order at the C5 region, which is reflected by the absence

of changes in the $S_{5\text{-SASL}}$ value and the absence of hysteresis in the $A_{\text{TMA-DPH}}$ heating–cooling cycle. Thus, PI seemed to operate in an all or none fashion affecting the membrane as a whole with catastrophic effects on the receptor including: (i) conformational change leading to inactive → active transformation, (ii) change in the relative accessibility of the binding sites, or (iii) protein receptor recruitment and trafficking involving phenomena such as the fusion of vesicle membranes containing $GABA_A$-R (r.f. [65]).

Cho Extraction Through β-CD Treatment (CD-PI)

Cho extraction in CD-PI induced a diminution of B_{max}, without changing the binding affinity with respect to CON-PI. The observed effect cannot be due to an underestimation of the B_{max} value resulting from β-CD interference with the method of protein quantification, or the sequestration of radioligand ([^{3}H]-FNZ) by the β-CD or the direct interaction of the β-CD with the FNZ binding site at the $GABA_A$-R. Unexpectedly, the CD-PI SM were less compressible even than the CON-PI. That effect was not only related to the possible interaction of β-CD with the membrane but also could be due to the compositional change, which was more complex than simple Cho elimination. The decrease in both Cho and phospholipids content was demonstrated (Table 1) and the loss of other membrane components cannot be excluded. Cho depletion induced a decrease in the molecular order within the region sensed by 5-SASL. The effect observed on the binding of [^{3}H]-FNZ (increase of B_{max}) after PI may be the result of a proper membrane annealing not achieved in the CON sample. Furthermore, the diminution of the order induced by the Cho extraction may have led to a reduced recruitment of specific binding sites. However, some effects related to the presence of residual amounts of β-CD in the membrane cannot be discarded. The increase in molecular order within the membrane core could correlate with an augmented molecular packing due a restructuring of membrane components usually associated with a decrease in surface hydration. The latter would favor the concentration of the hydrophobic ligand FNZ near a hydrophobic binding site at $GABA_A$-R (as proposed previously [25]). Although, an increase in surface hydration upon Cho depletion were claimed from experiments with the 3-hydroxyflavone derivative hydration probe (liquid-ordered and liquid-disordered phases are less hydrated than the liquid crystalline phase [66]), a reduction in Laurdan generalized polarization [67] was reported. Moreover, it has been recognized that there are some Cho concentrations at which Laurdan spectral properties changes discontinuously. This and other findings (see "Steady-state fluorescence of DPH and TMA-DPH" section) points to the concept that the relationship between Cho content and membrane organization/hydration is non-linear and, at some extent may become unpredictable.

Furthermore, the correlation between ordering at the membrane core and disruption of the water surface network is illustrated by the EPR results obtained before and after the binding of the polyhydroxylated mycotoxin fumonisin B1 to phospholipid vesicles [68]. Moreover, a restructuring of membrane components may lead to a reduction in membrane curvature which may facilitate endocytosis and membrane receptor cycling as shown in living cells [7].

It has been reported that the $GABA_A$-Rs are mainly localized in clusters within condensed domains known as lipid rafts, both in cell bodies and neurites [69]. On the other hand, experiments with two-photon microscopy suggested that changes in cellular Cho content affect the entire membrane rather than being localized in specific macroscopic domains [58]. Hence, β-CD treatments may have affected the whole equilibrium phase organization at the membrane surface, including microdomain organization of proteins, and also influence functional protein–lipid interactions.

Our results on the thermally and compositionally induced changes in membrane order at different depths are summarized in Fig. 8.

Conclusions

The treatment of the SM with β-CD for Cho extraction implied a PI at 37°C that would facilitate a reorganization of membrane components allowing the recruitment of receptor sites. In CD-PI samples, fewer sites would be exposed (with respect to the CON-PI) as a result of the change in membrane composition (the β-CD would extract Cho, phospholipids, and proteins [45, 48]) as well as the eventual adsorption of β-CD to the membrane.

In this study, we have demonstrated that the use of β-CD for Cho depletion or enrichment in SMs must be carefully used, since the effects observed after membrane treatment with β-CD cannot be rationalized as a simple change in Cho content because the latter is accompanied by a complex change in membrane composition, an irreversible effect induced by temperature cycling on membrane organization and, possibly, also by residual β-CD amounts that remain adsorbed, due to the impossibility of their being totally eliminated from the system by means of centrifugation washings. In addition, β-CD was able to interact with all the probes tested which highlights the

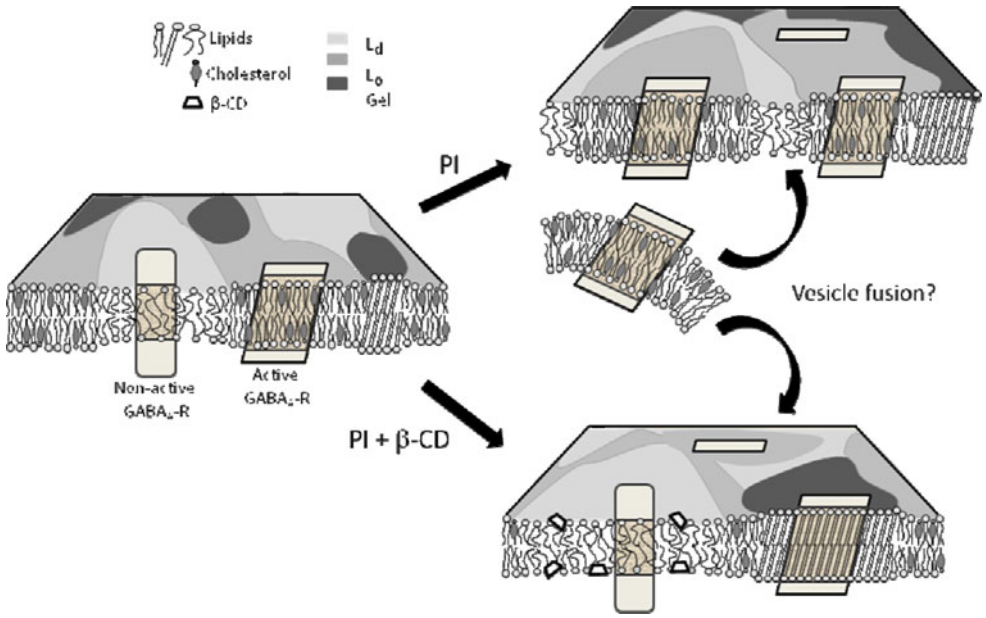

Fig. 8 Hypothetical model of membrane changes upon PI and β-CD treatment. The PI treatment is a source of perturbation. β-CD induced a change in membrane composition including Cho extraction increasing the proportion of liquid-disordered phase. PI, with or without β-CD, change the whole equilibrium phase organization of the membrane, modified microdomain organization of proteins and functional protein–lipid interactions affecting receptor conformation and activity. The model suggests that the active receptor can be found in the more ordered phases (either gel of liquid ordered). PI with or without β-CD induces a $GABA_A$-R recruitment possibly through membrane trafficking (vesicle fusion) or other unknown mechanisms. Some β-CD molecules are partitioned within the polar head group. *Lo* liquid ordered, *Ld* liquid disordered

importance of a careful data analysis to achieved meaningful conclusions.

Acknowledgments This study was partially financed by Grants from CONICET, SECyT-Universidad Nacional de Córdoba, Mincyt-Pcia.Córdoba and ANPCyT from Argentina and Fundacão de Amparo à Pesquisa do Estado de São Paulo, Brasil. A.V.T. and M.A.P. are Career Investigators from CONICET, Argentina. S.S. holds a research fellowship from Conselho Nacional de Desenvolvimento Científico e Tecnológico, Brasil.

References

1. Lundbaek, J. A., et al. (1996). Membrane stiffness and channel function. *Biochemistry, 35*(12), 3825–3830.
2. Whetton, A. D., Gordon, L. M., & Houslay, M. D. (1983). Adenylate cyclase is inhibited upon depletion of plasma-membrane cholesterol. *Biochemical Journal, 212*(2), 331–338.
3. North, P., & Fleischer, S. (1983). Alteration of synaptic membrane cholesterol/phospholipid ratio using a lipid transfer protein. Effect on gamma-aminobutyric acid uptake. *Journal of Biological Chemistry, 258*(2), 1242–1253.
4. Gimpl, G., Burger, K., & Fahrenholz, F. (1997). Cholesterol as modulator of receptor function. *Biochemistry, 36*(36), 10959–10974.
5. Jafurulla, M., Tiwari, S., & Chattopadhyay, A. (2011). Identification of cholesterol recognition amino acid consensus (CRAC) motif in G-protein coupled receptors. *Biochemical and Biophysical Research Communications, 404*(1), 569–573.
6. Antollini, S. S., & Barrantes, F. J. (1998). Disclosure of discrete sites for phospholipid and sterols at the protein–lipid interface in native acetylcholine receptor-rich membrane. *Biochemistry, 37*(47), 16653–16662.
7. Borroni, V., et al. (2007). Cholesterol depletion activates rapid internalization of submicron-sized acetylcholine receptor domains at the cell membrane. *Molecular Membrane Biology, 24*(1), 1–15.
8. Pucadyil, T. J., & Chattopadhyay, A. (2004). Cholesterol modulates ligand binding and G-protein coupling to serotonin(1A) receptors from bovine hippocampus. *Biochimica et Biophysica Acta, 1663*(1–2), 188–200.
9. Pucadyil, T. J., & Chattopadhyay, A. (2005). Cholesterol modulates the antagonist-binding function of hippocampal serotonin1A receptors. *Biochimica et Biophysica Acta, 1714*(1), 35–42.
10. Klein, U., Gimpl, G., & Fahrenholz, F. (1995). Alteration of the myometrial plasma membrane cholesterol content with beta-cyclodextrin modulates the binding affinity of the oxytocin receptor. *Biochemistry, 34*(42), 13784–13793.
11. Barrantes, F. J. (2004). Structural basis for lipid modulation of nicotinic acetylcholine receptor function. *Brain Research Brain Research Reviews, 47*(1–3), 71–95.
12. Sooksawate, T., & Simmonds, M. A. (2001). Influence of membrane cholesterol on modulation of the GABA(A) receptor by neuroactive steroids and other potentiators. *British Journal of Pharmacology, 134*(6), 1303–1311.
13. Bennett, P. J., & Simmonds, M. A. (1996). The influence of membrane cholesterol on the $GABA_A$ receptor. *British Journal of Pharmacology, 117*(1), 87–92.
14. Kilsdonk, E. P., et al. (1995). Cellular cholesterol efflux mediated by cyclodextrins. *Journal of Biological Chemistry, 270*(29), 17250–17256.

15. Christian, A., et al. (1997). Use of cyclodextrins for manipulating cellular cholesterol content. *Journal of Lipid Research, 38*(11), 2264–2272.
16. Agarwal, S. R., et al. (2011). Effects of cholesterol depletion on compartmentalized cAMP responses in adult cardiac myocytes. *Journal of Molecular and Cellular Cardiology, 50*(3), 500–509.
17. Szente, L., & Szejtli, J. (1999). Highly soluble cyclodextrin derivatives: Chemistry, properties, and trends in development. *Advanced Drug Delivery Reviews, 36*(1), 17–28.
18. Duchene, D., Ponchel, G., & Wouessidjewe, D. (1999). Cyclodextrins in targeting. Application to nanoparticles. *Advanced Drug Delivery Reviews, 36*(1), 29–40.
19. Hirayama, F., & Uekama, K. (1999). Cyclodextrin-based controlled drug release system. *Advanced Drug Delivery Reviews, 36*(1), 125–141.
20. Mishur, R. J., et al. (2011). Molecular recognition and enhancement of aqueous solubility and bioactivity of CD437 by beta-cyclodextrin. *Bioorganic & Medicinal Chemistry Letters, 21*(2), 857–860.
21. Jablin, M. S., et al. (2010). Effects of beta-cyclodextrin on the structure of sphingomyelin/cholesterol model membranes. *Biophysical Journal, 99*(5), 1475–1481.
22. Camilleri, P., Haskins, N. J., & Howlett, D. R. (1994). beta-Cyclodextrin interacts with the Alzheimer amyloid beta-A4 peptide. *FEBS Letters, 341*(2–3), 256–258.
23. Pytel, M., Mercik, K., & Mozrzymas, J. W. (2006). Interaction between cyclodextrin and neuronal membrane results in modulation of GABA(A) receptor conformational transitions. *British Journal of Pharmacology, 148*(4), 413–422.
24. Sogaard, R., et al. (2006). GABA(A) receptor function is regulated by lipid bilayer elasticity. *Biochemistry, 45*(43), 13118–13129.
25. Garcia, D. A., Marin, R. H., & Perillo, M. A. (2002). Stress-induced decrement in the plasticity of the physical properties of chick brain membranes. *Molecular Membrane Biology, 19*(3), 221–230.
26. Zasadzinski, J. A., et al. (1994). Langmuir–Blodgett films. *Science, 263*(5154), 1726–1733.
27. Perillo, M. A., & Arce, A. (1991). Determination of the membrane–buffer partition coefficient of flunitrazepam, a lipophilic drug. *Journal of Neuroscience Methods, 36*(2–3), 203–208.
28. Niu, S. L., & Litman, B. J. (2002). Determination of membrane cholesterol partition coefficient using a lipid vesicle-cyclodextrin binary system: Effect of phospholipid acyl chain unsaturation and headgroup composition. *Biophysical Journal, 83*(6), 3408–3415.
29. Lowry, O. H., et al. (1951). Protein measurement with the Folin phenol reagent. *Journal of Biological Chemistry, 193*(1), 265–275.
30. Yammamura, H. I., Enna, S. J., & Michael, J. K. (1978). *Neurotransmiter receptor binding*. New York: Raven.
31. Esmann, M., & Marsh, D. (1985). Spin-label studies on the origin of the specificity of lipid–protein interactions in Na+, K+-ATPase membranes from *Squalus acanthias*. *Biochemistry, 24*(14), 3572–3578.
32. Sanson, A., et al. (1976). An ESR study of the anchoring of spin-labeled stearic acid in lecithin multilayers. *Chemistry and Physics of Lipids, 17*(4), 435–444.
33. Egret-Charlier, M., Sanson, A., & Ptak, M. (1978). Ionization of fatty acids at the lipid–water interface. *FEBS Letters, 89*(2), 313–316.
34. Jost, P. C., et al. (1973). Evidence for boundary lipid in membranes. *Proceedings of the National Academy of Sciences of the United States of America, 70*(2), 480–484.
35. Schreier, S., Polnaszek, C. F., & Smith, I. C. (1978). Spin labels in membranes. Problems in practice. *Biochimica et Biophysica Acta, 515*(4), 395–436.
36. Hoffman, P., Sandhoff, K., & Marsh, D. (2000). Comparatie dynamics and location of chain spin-labelled sphingomyelin and phosphatidylcholine in dimyristoyl phosphatidylcholine membranes studied by EPR spectroscopy. *Biochimica et Biophysica Acta, 1468*, 359–366.
37. Szabo, A.G. (2000). Fluorescence principles and measurements. In M. G. Gore (Ed.) *Spectrophotometry and spectrofluorimetry*. Oxford: Oxford University Press.
38. Ruan, K., & Balny, C. (2002). High pressure static fluorescence to study macromolecular structure–function. *Biochimica et Biophysica Acta, 1595*(1–2), 94–102.
39. Silva, J. L., Miles, E. W., & Weber, G. (1986). Pressure dissociation and conformational drift of the beta dimer of tryptophan synthase. *Biochemistry, 25*(19), 5780–5786.
40. Lackowicz, R. J. (1983). *Principles of fluorescence spectroscopy*. New York: Plenum Press.
41. Verger, R., & Pattus, F. (1976). Spreading of membranes at the air/water interface. *Chemistry and Physics of Lipids, 16*(4), 285–291.
42. Rosetti, C. M., Maggio, B., & Oliveira, R. G. (2008). The self-organization of lipids and proteins of myelin at the membrane interface. Molecular factors underlying the microheterogeneity of domain segregation. *Biochimica et Biophysica Acta, 1778*(7–8), 1665–1675.
43. Sokal, R., & Rohlf, F. (1987). Introduction to biostatistics. A series of books in biology. New York: W. H. Freeman & Company.
44. Absalom, N. L., Lewis, T. M., & Schofield, P. R. (2004). Mechanisms of channel gating of the ligand-gated ion channel superfamily inferred from protein structure. *Experimental Physiology, 89*(2), 145–153.
45. Irie, T., & Uekama, K. (1999). Cyclodextrins in peptide and protein delivery. *Advanced Drug Delivery Reviews, 36*(1), 101–123.
46. Cabeca, L. F., et al. (2008). Topology of a ternary complex (proparacaine-beta-cyclodextrin-liposome) by STD NMR. *Magnetic Resonance in Chemistry, 46*(9), 832–837.
47. Breckenridge, W. C., Gombos, G., & Morgan, I. G. (1972). The lipid composition of adult rat brain synaptosomal plasma membranes. *Biochimica et Biophysica Acta, 266*(3), 695–707.
48. Ohtani, Y., et al. (1989). Differential effects of alpha-, beta- and gamma-cyclodextrins on human erythrocytes. *European Journal of Biochemistry, 186*(1–2), 17–22.
49. Oliveira, R. G., Calderon, R. O., & Maggio, B. (1998). Surface behavior of myelin monolayers. *Biochimica et Biophysica Acta, 1370*(1), 127–137.
50. Feng, S.-S. (1999). Interpretation of mechanochemical properties of lipid bilayer vesicles from the equation of state or pressure–area measurement of the monolayer at the air–water or oil–water interface. *Langmuir, 15*(4), 998–1010.
51. Cassera, M. B., Silber, A. M., & Gennaro, A. M. (2002). Differential effects of cholesterol on acyl chain order in erythrocyte membranes as a function of depth from the surface. An electron paramagnetic resonance (EPR) spin label study. *Biophysical Chemistry, 99*(2), 117–127.
52. Rossi, S., et al. (2007). Self-assembly of beta-cyclodextrin in water. 2. Electron spin resonance. *Langmuir, 23*(22), 10959–10967.
53. Sanchez, J. M., Turina, A. V., & Perillo, M. A. (2007). Spectroscopic probing of ortho-nitrophenol localization in phospholipid bilayers. *Journal of Photochemistry and Photobiology B, 89*(1), 56–62.
54. Garcia, D. A., & Perillo, M. A. (2002). Flunitrazepam-membrane non-specific binding and unbinding: Two pathways with different energy barriers. *Biophysical Chemistry, 95*(2), 157–164.
55. Mukherjee, S., & Chattopadhyay, A. (2005). Monitoring the organization and dynamics of bovine hippocampal membranes

utilizing Laurdan generalized polarization. *Biochimica et Biophysica Acta, 1714*(1), 43–55.
56. Mukherjee, S., et al. (2007). Dynamics and heterogeneity of bovine hippocampal membranes: Role of cholesterol and proteins. *Biochimica et Biophysica Acta, 1768*(9), 2130–2144.
57. Harris, F. M., Best, K. B., & Bell, J. D. (2002). Use of Laurdan fluorescence intensity and polarization to distinguish between changes in membrane fluidity and phospholipid order. *Biochimica et Biophysica Acta, 1565*(1), 123–128.
58. Stott, B. M., et al. (2008). Use of fluorescence to determine the effects of cholesterol on lipid behavior in sphingomyelin liposomes and erythrocyte membranes. *Journal of Lipid Research, 49*(6), 1202–1215.
59. Wilson-Ashworth, H. A., et al. (2006). Differential detection of phospholipid fluidity, order, and spacing by fluorescence spectroscopy of bis-pyrene, prodan, nystatin, and merocyanine 540. *Biophysical Journal, 91*(11), 4091–4101.
60. Wang, M. M., Sugar, I. P., & Chong, P. L. (1998). Role of the sterol superlattice in the partitioning of the antifungal drug nystatin into lipid membranes. *Biochemistry, 37*(34), 11797–11805.
61. Chong, P. L. (1994). Evidence for regular distribution of sterols in liquid crystalline phosphatidylcholine bilayers. *Proceedings of the National Academy of Sciences of the United States of America, 91*(21), 10069–10073.
62. Zidovetzki, R., & Levitan, I. (2007). Use of cyclodextrins to manipulate plasma membrane cholesterol content: Evidence, misconceptions and control strategies. *Biochimica et Biophysica Acta, 1768*(6), 1311–1324.
63. Li, G., & McGown, L. B. (1994). Molecular nanotube aggregates of beta- and gamma-cyclodextrins linked by diphenylhexatrienes. *Science, 264*(5156), 249–251.
64. Disalvo, E. A., et al. (2002). Physical chemistry of lipid interfaces: State of hydration, topological and electrical properties. In C. A. Condat & A. Baruzzi (Eds.), *Resent research developements in Biophysical Chemistry* (pp. 181–197). Kerala: Research Signpost.
65. Benavidez, E., & Arce, A. (2002). Effects of phosphorylation and cytoskeleton-affecting reagents on GABA(A) receptor recruitment into synaptosomes following acute stress. *Pharmacology, Biochemistry and Behavior, 72*(3), 497–506.
66. M'Baye, G., et al. (2008). Liquid ordered and gel phases of lipid bilayers: Fluorescent probes reveal close fluidity but different hydration. *Biophysical Journal, 95*(3), 1217–1225.
67. Parasassi, T., et al. (1994). Cholesterol modifies water concentration and dynamics in phospholipid bilayers: A fluorescence study using Laurdan probe. *Biophysical Journal, 66*(3 Pt 1), 763–768.
68. Yin, J. J., et al. (1996). Effects of fumonisin B1 and (hydrolyzed) fumonisin backbone AP1 on membranes: A spin-label study. *Archives of Biochemistry and Biophysics, 335*, 13–22.
69. Dalskov, S., et al. (2005). Lipid raft localization of $GABA_A$ receptor and Na+, K+-ATPase in discrete microdomain clusters in rat cerebellar granule cells. *Neurochemistry International, 46*, 489–499.